3 Error Equations for Blind Equalization Schemes

In this section different error equations for blind equalization will be analyzed. Based on this analysis a suitable error equation will be suggested aimed at providing better performance. The model of the equalizer used for the error analysis is given in Figure 2.1. For convenience that same figure is also shown in Figure 3.1. As mentioned in the previous chapter, in a blind equalization scheme, instead of using a training sequence, some statistical property of the signal is used for the determination of the instantaneous error, *e(n)*, which is then used for updating the equalizer coefficient vector **f**(n).

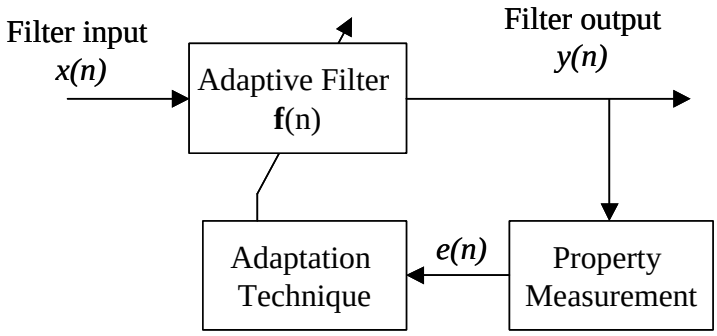

Figure 3.1: Adaptive Filter Model for Blind Equalization.

Generally, the constant modularity of the output signal $y(n)$ is the desired property, which needs to be restored. The adaptive algorithm that works mainly to restore the constant modulus property of the output signal is known as the *Constant Modulus Algorithm* (CMA), and the same algorithm will be used to analyze the properties of different error equations. Error equations used in the *property measurement* block of Figure 3.1 measure the deviation of the output signal amplitude from the desired amplitude level and force the adaptive algorithm to change the equalizer coefficients to compensate for the present error. How much the adaptive algorithm will compensate for a specific deviation of the output signal amplitude from the desired amplitude level is completely dependent on the error equation. Therefore the error equation used in an adaptive system exercises significant control over the overall

system performance. In the following sections four different types of error equation will be defined and analyzed.

3.1 Error Signals

Out of the many possible error equations the following are selected for analysis. The first three equations were suggested earlier [8].

$$\begin{aligned}
&\text{Type1}: \; e(n) = |y(n)|^2 - A^2 \\
&\text{Type2}: \; e(n) = |y(n)| - A \\
&\text{Type3}: \; e(n) = \ln\left(\frac{|y(n)|}{A}\right) \\
&\text{Type4}: \; e(n) = \begin{cases} \sqrt{|y(n)|^2 - A^2}, & \text{if } |y(n)| > A \\ -\sqrt{A^2 - |y(n)|^2}, & \text{if } |y(n)| < A \end{cases}
\end{aligned} \tag{3.1}$$

In (3.1), *A* is the desired amplitude level. All the selected error equations are non-linear and this non-linearity of the error equation causes the blind equalization scheme to be non-linear. All of the error equations become zero when the amplitude of *y(n)* has the proper value. They also provide sign information to indicate whether the absolute value of *y(n)* is less than or greater than the desired value *A*. This sign information determines the direction of adaptation, i.e. whether the present values of the filter coefficients need to be increased or decreased. Figure 3.2 shows how the error varies with the absolute value of the filter output *y(n)* for the different error types. A desired output amplitude of 1 (one) was used in plotting the error curves.

Type1 is the most commonly used error equation with CMA based blind equalization. Therefore the blind equalization scheme that uses the Type1 error equation with a *fractionally spaced equalizer* (FSE) will be named the "*Conventional Blind Equalizer*" and this scheme will be used throughout the report for comparison purposes.

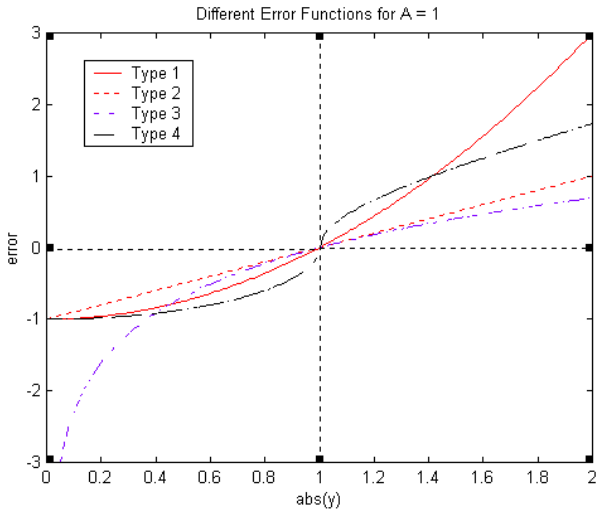

Figure 3.2: Different Types of Error Functions.

The adaptive algorithm with a Type1 error equation will compensate more when the amplitude level of the output signal is higher than the desired amplitude level. This kind of compensation will result in a better convergence rate at the beginning of the adaptation process since, in this situation generally, the error signal has a large positive value. However, near the convergence point, for the same positive and negative deviations of the amplitude level from its desired value, the Type1 error does not provide the same compensation. Due to this non-symmetric behavior of the error equation, with Type1 error, the convergence rate adjacent to the minimum may not be as good as near the beginning of the adaptation process. Recall that, for Type1 error, the value of the error increases exponentially with the amplitude deviation. Therefore, noise spikes may cause the equalizer to deviate from a stable solution.

The error equation of Type2 has an affine relation with the amplitude of the equalizer output and is symmetric about zero error. Due to the symmetric nature, unlike for a Type1 error, a Type2 error results in the same amount of compensation for the same amount of deviation of the output amplitude from the desired value, irrespective of the sign of the deviation. The sign only determines the direction of the compensation. For this reason with this error equation type, the steady state performance is expected to be better than with Type1. The convergence rate with a Type2 error equation may not be as good as for Type1 at

the beginning of the adaptation process if the envelope of the equalizer output has a much higher value than the desired amplitude level.

The adaptation process with a Type3 error equation is expected to behave the same as for Type2 adjacent to minima of the cost surface, due to the symmetric nature of the cost surface near the global minimum. However, a Type3 error may cause a worse convergence rate at the beginning of the adaptation process. Again, this type of error is very sensitive to noise, like a Type1 error, but in the opposite direction, i.e., when the equalizer output amplitude becomes too small. Moreover, this is the only type of error (Section 3.2.3), for which the output signal appears in the denominator of the weight update equation. Therefore, if the output becomes zero for some reason (perhaps due to noise) the equalizer may begin to diverge. This problem can be avoided by not allowing the output to go below a certain predefined level.

The Type4 error equation is designed to avoid the sensitivity to noise and also to provide a better convergence rate at the beginning of the adaptation process. The Type4 error is also symmetric about zero adjacent to the minimum point of the cost surface. However, near the convergence point, the Type4 error results in a higher value than any of the other error types. For this reason, the steady state noise floor for the Type4 error is expected to be higher than that for any other error type.

Since the method of calculating the error signal determines the equations for updating the adaptive filter coefficients (or tap weights), the weight update equations for different types of error will be derived in the next section. Again, for any of the above types of error, the system becomes non-linear and analytically intractable. Therefore simulation results will be used to compare the adaptation rate for the different types of error equation. The update equations, derived in the next section, will be used in the simulation.

3.2 Weight Update Equations

Updating the coefficients of the filter (tap weights for linear transversal filter) is aimed at optimization of the cost function. The cost function is generally a function of the error signal $e(n)$ and denoted as $J[e(n)]$. The cost function $J[e(n)]$ should have the following characteristics [3]:

$$\begin{aligned} &\text{a)} \quad 0 \le J\left[e(n)\right] = J\left[-e(n)\right] \\ &\text{b)} \quad \text{if } 0 \le e(1) \le e(2),\ J\left[e(1)\right] \le J\left[e(2)\right] \end{aligned} \tag{3.2}$$

The most commonly used cost function is the expected value of the square of the error signal. Thus the objective of the adaptive algorithm is to minimize the mean square error. For simplicity of calculation, the same cost function will be used to derive the weight update equations.

$$J\left[e(n)\right] = E\left\{e^2(n)\right\} \tag{3.3}$$

$E\{\bullet\}$ in (3.3) is the statistical expectation operator. Thus $J[e(n)]$ is the mean square of the error sensed in measuring adherence to the constant envelope property. The constant modulus algorithm (CMA) employs the approximate gradient descent method to minimize the cost function given in (3.3), and the update equation for the filter coefficients becomes,

$$\mathbf{f}(n+1) = \mathbf{f}(n) - \mu \nabla_{\mathbf{f}} J \tag{3.4}$$

In (3.4), $\mathbf{f}(n) = [f(0)\ f(1)\ f(2)\ \ldots\ f(N\text{-}1)]^T$ is the filter tap weight vector at instant n, and μ is the adaptation step size, which is a small positive number. The true gradient in (3.4), at instant n, is approximated by its instantaneous value and the notation is changed to $\hat{\nabla}_{\mathbf{f}}$.

$$\begin{aligned} \hat{\nabla}_{\mathbf{f}} J &= \frac{\partial}{\partial \mathbf{f}(n)}\left\{e^2(n)\right\} \\ &= 2e(n)\frac{\partial e(n)}{\partial \mathbf{f}(n)} \end{aligned} \tag{3.5}$$

Now the weight update equations (3.4) will be derived for the different types of error given in (3.1).

3.2.1 Type1

$$e(n) = |y(n)|^2 - A^2 = y^*(n)y(n) - A^2 \tag{3.6}$$

Here $y^*(n)$ is the conjugate of the output of the filter $y(n)$. To evaluate (3.5) for the Type1 error, $y(n)$ needs to be expressed in terms of $\mathbf{f}(n)$. A complex system will be assumed in the derivation.

$$y(n) = \sum_{l=0}^{N-1} f^*(n,l)x(n-l) = \mathbf{f}^H(n)\mathbf{x}(n) \tag{3.7}$$

In (3.7), $\mathbf{f}^H(n)$ is the complex conjugate transpose of the filter coefficient vector (tap weight vector) $\mathbf{f}(n)$ and $\mathbf{x}(n) = [x(n)\ \ x(n-1)\ \ x(n-2)\cdots x(n-N+1)]^T$ is the input vector to the equalizer (adaptive filter) at instant n. N is the filter length. Now,

$$\begin{aligned}
\hat{\nabla}_{\mathbf{f}} J &= 2e(n)\frac{\partial e(n)}{\partial \mathbf{f}(n)} \\
&= 2e(n)\frac{\partial}{\partial \mathbf{f}(n)}\left\{y(n)y^*(n) - A^2\right\} \\
&= 2e(n)\frac{\partial}{\partial \mathbf{f}(n)}\left\{y(n)y^*(n)\right\} \\
&= 2e(n)\frac{\partial}{\partial \mathbf{f}(n)}\left\{\mathbf{f}^H(n)\mathbf{x}(n)\mathbf{x}^H(n)\mathbf{f}(n)\right\} \\
&= 2e(n)\frac{\partial}{\partial \mathbf{f}(n)}\left\{\mathbf{f}^H(n)\mathbf{A}(n)\mathbf{f}(n)\right\}
\end{aligned} \tag{3.8}$$

Here, $\mathbf{A}(n) = \mathbf{x}(n)\mathbf{x}^H(n)$. Therefore,

$$\begin{aligned}
\hat{\nabla}_{\mathbf{f}} J &= 4e(n)\mathbf{A}(n)\mathbf{f}(n) \\
&= 4e(n)\mathbf{x}(n)y^*(n)
\end{aligned} \tag{3.9}$$

Substituting $\nabla_{\mathbf{f}} J$ in (3.4) by $\hat{\nabla}_{\mathbf{f}} J$, the weight update equation for Type1 error can be written as:

$$\mathbf{f}(n+1) = \mathbf{f}(n) - \mu\, e(n) y^*(n) \mathbf{x}(n) \tag{3.10}$$

In (3.10) all the constants are lumped together into the single constant μ, the step size of the adaptation process. The same will be done for the other types of error equation.

3.2.2 Type2

$$e(n) = |y(n)| - A = \sqrt{y(n) y^*(n)} - A \tag{3.11}$$

The gradient of the cost function,

$$\begin{aligned} \hat{\nabla}_{\mathbf{f}} J &= 2e(n) \frac{\partial e(n)}{\partial \mathbf{f}(n)} \\ &= 2e(n) \frac{\partial}{\partial \mathbf{f}(n)} \left\{ \sqrt{y(n) y^*(n)} - A^2 \right\} \\ &= 2e(n) \frac{2 y^*(n) \mathbf{x}(n)}{2\sqrt{y(n) y^*(n)}} \\ &= 2e(n) \frac{y^*(n) \mathbf{x}(n)}{|y(n)|} \end{aligned} \tag{3.12}$$

The weight update equation can be obtained from (3.4) by replacing the value of $\hat{\nabla}_{\mathbf{f}} J$. Therefore,

$$\mathbf{f}(n+1) = \mathbf{f}(n) - \mu\, e(n) \frac{y^*(n) \mathbf{x}(n)}{|y(n)|} \tag{3.13}$$

3.2.3 Type3

$$e(n) = \ln\left(\frac{|y(n)|}{A} \right) = \frac{1}{2} \ln\left(\frac{|y(n)|^2}{A^2} \right) \tag{3.14}$$

The gradient of the cost function,

$$\begin{aligned}\hat{\nabla}_{\mathbf{f}} J &= 2e(n)\frac{\partial e(n)}{\partial \mathbf{f}(n)} \\ &= e(n)\frac{\partial}{\partial \mathbf{f}(n)}\left\{\ln\left(\frac{|y(n)|^2}{A^2}\right)\right\} \\ &= e(n)\frac{\partial}{\partial \mathbf{f}(n)}\left\{\ln\left(|y(n)|^2\right)\right\} \\ &= e(n)\frac{1}{|y(n)|^2}\frac{\partial}{\partial \mathbf{f}(n)}\left\{|y(n)|^2\right\} \\ &= e(n)\frac{y^*(n)\mathbf{x}(n)}{|y(n)|^2}\end{aligned} \tag{3.15}$$

The weight update equation from (3.4),

$$\mathbf{f}(n+1) = \mathbf{f}(n) - me(n)\frac{\mathbf{x}(n)}{y(n)} \tag{3.16}$$

3.2.4 Type4

$$e(n) = \begin{cases} \sqrt{|y(n)|^2 - A^2}, & \text{if } |y(n)| > A \\ -\sqrt{A^2 - |y(n)|^2}, & \text{if } |y(n)| < A \end{cases} \tag{3.17}$$

Case 1: $e(n) = \sqrt{|y(n)|^2 - A^2}, \qquad \text{if } |y(n)| > A$

$$\begin{aligned}\hat{\nabla}_{\mathbf{f}} J &= 2e(n)\frac{\partial e(n)}{\partial \mathbf{f}(n)} \\ &= 2e(n)\frac{\partial}{\partial \mathbf{f}(n)}\left\{\sqrt{|y(n)|^2 - A^2}\right\} \\ &= 2e(n)\frac{1}{2\sqrt{|y(n)|^2 - A^2}}\frac{\partial}{\partial \mathbf{f}(n)}\left\{|y(n)|^2\right\} \\ &= 2y^*(n)\mathbf{x}(n)\end{aligned} \tag{3.18}$$

Case 2: $e(n) = -\sqrt{A^2 - |y(n)|^2}$, if $|y(n)| < A$

$$\begin{aligned}\hat{\nabla}_{\mathbf{f}} J &= 2e(n)\frac{\partial e(n)}{\partial \mathbf{f}(n)} \\ &= -2e(n)\frac{\partial}{\partial \mathbf{f}(n)}\left\{\sqrt{A^2 - |y(n)|^2}\right\} \\ &= 2e(n)\frac{1}{2\sqrt{A^2 - |y(n)|^2}}\frac{\partial}{\partial \mathbf{f}(n)}\left\{|y(n)|^2\right\} \\ &= -2y^*(n)\mathbf{x}(n)\end{aligned} \tag{3.19}$$

In general, the gradient can be represented as:

$$\hat{\nabla}_{\mathbf{f}} J = 2sign\big(|y(n)| - A\big)y^*(n)\mathbf{x}(n). \tag{3.20}$$

Therefore the weight update equation for the Type4 error is:

$$\mathbf{f}(n+1) = \mathbf{f}(n) - m\ sign\big(|y(n)| - A\big)y^*(n)\mathbf{x}(n) \tag{3.21}$$

To make it similar to the Normalized Least Mean Square Algorithm (NLMS), the weight update equations for the different types of error signals were reformulated and the new (normalized) update equations are shown in Table 3.1. These equations were used in the simulations to update the coefficients of the *Fractionally Spaced Equalizer* (FSE).

Table 3.1: Weight Update Equations for Different Error Types.

Type1:	$\mathbf{f}(n+1) = \mathbf{f}(n) - \dfrac{m\,e(n)y^*(n)\mathbf{x}(n)}{\|\mathbf{x}(n)\|^2}$	(3.22)
Type2:	$\mathbf{f}(n+1) = \mathbf{f}(n) - m\,e(n)\dfrac{y^*(n)\mathbf{x}(n)}{\|y(n)\|\|\mathbf{x}(n)\|^2}$	(3.23)
Type3:	$\mathbf{f}(n+1) = \mathbf{f}(n) - m\,e(n)\dfrac{\mathbf{x}(n)}{y(n)\|\mathbf{x}(n)\|^2}$	(3.24)
Type4:	$\mathbf{f}(n+1) = \mathbf{f}(n) - \dfrac{m\,sign\big(\|y(n)\| - A\big)y^*(n)\mathbf{x}(n)}{\|\mathbf{x}(n)\|^2}$	(3.25)

3.3 Simulation Results

Simulations were performed to determine the convergence rate of the system for the different types of error signals. A Fractionally Spaced Equalizer (FSE) with an over-sampling factor of 3 (M = 3) was used in the simulation. For simplicity, BPSK modulation was used in the simulation. The block diagram of the simulated system is shown in Figure 3.3.

The *fractionally spaced equalizer* (FSE) of Figure 3.3 is an adaptive equalizer and its functional diagram is shown in Figure 3.1. The only difference between the implemented equalizer and the one in Figure 3.1 is that, in the simulation, the equalizer coefficients were updated for every Mth (M is the over-sampling factor of the equalizer) output sample. This is due to the fact that the FSE requires M samples to make a decision for a single output. For this reason, in Figure 3.3, the FSE and the down sampler are shown in the same block.

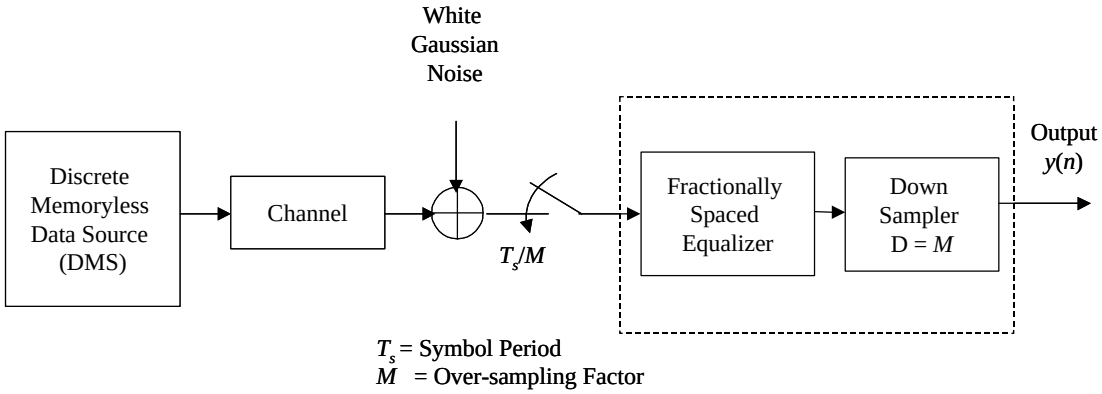

Figure 3.3: Block Diagram of Simulated System Used for Analysis of Different Error Signals.

Since the main objective here is to analyze the convergence properties and the steady state performance of the blind equalization schemes for different error types, all simulations were performed with external noise. The *signal-to-noise ratio* (SNR) used in the simulation was 40 dB for all experiments. To observe how each of the error equations affects the convergence rate of the equalizer under different channel conditions, different types of channels were used in the simulation. All the implemented channels are of the same length (3 in baud space) but have different frequency responses. Recall that in Section 2.1.1 it has been

shown that the whole system with FSE can be decomposed into multiple channels, where the number of sub-channels is the same as the over-sampling factor *M*. It is also shown in Section 2.1.2 that to have a perfect equalizer, the sub-channels (baud spaced) of all of the paths should not have common zeros. For this purpose, an extra zero was inserted (at time index *k*=6 in fractional space) for all the channels while converting the baud space channel to the fractional space channel. This extra zero makes the channel length equal to 10 in fractional space.

In Section 2.1.3 it has been shown that, if the length of the channel (fractional space) and the equalizer are *ML* and *MN*, then for perfect source recovery, *N* should satisfy the following condition:

$$N \geq \frac{L-1}{M-1} \tag{3.26}$$

In (3.26), *M* is the over-sampling factor. Therefore, for a channel of length 10 (in fractional space), and an over-sampling factor of 3, the length of the FSE should be at least $3\left\lceil \frac{10/3-1}{3-1} \right\rceil = 6$. The length of the equalizer (FSE) used in the simulation was 12. The results of the simulation will be presented separately for different channels.

3.3.1 Minimum Phase Channel with Two Impulses

The channel impulse responses, both in baud space and in fractional space, are shown in Figure 3.4. For simplicity, rectangular pulse shaping was used in the simulation. The same pulse shaping will be used for all the channels unless specifically mentioned otherwise. Since the delay associated with the total system needs to be specified while initializing the blind equalizer, the group delay of the system is set to 1 for this specific channel. The *Mean Squared Error* (MSE) curves for the system with different error equations, while adapting the equalizer for the minimum phase channel with two impulses, are shown in Figure 3.5. Figure 3.6, which focuses on the initial adaptation process, is a zoomed version of Figure 3.5.

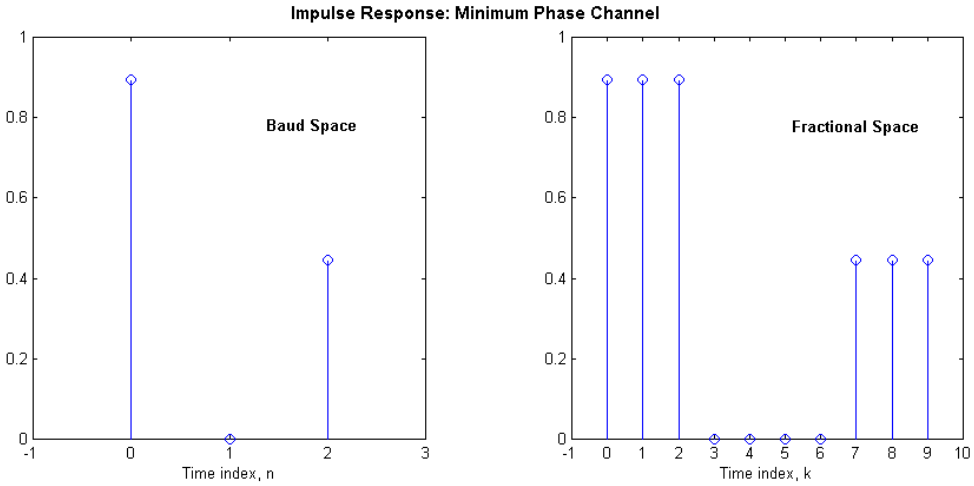

Figure 3.4: Impulse Response of the Minimum Phase Channel with Two Impulses.

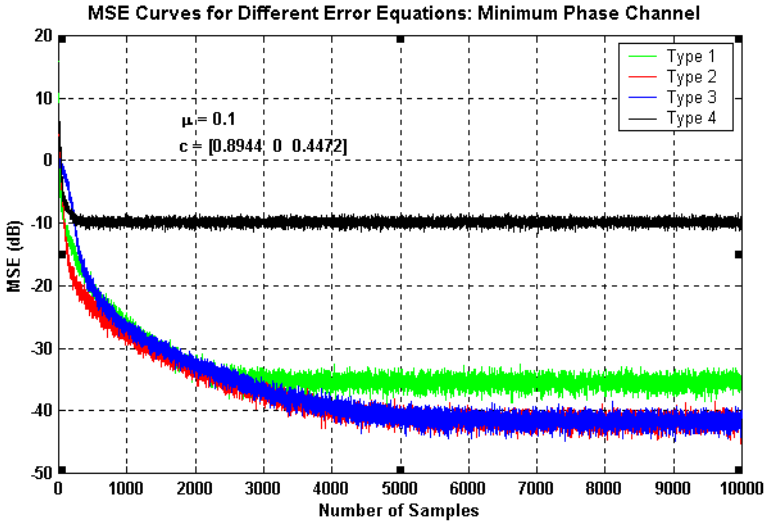

Figure 3.5: MSE Curves for Different Error Equations for the Channel Shown in Figure 3.4.

Figure 3.5 shows that, even though the system has an SNR of 40 dB, the MSE curves go below –40 dB for the Type2 and Type3 error equations. This is because, in these cases, the equalizer not only removes the ISI from the received symbols but also provides a spectral shaping of the white external noise. Due to this spectral shaping effect, the energy of the noise at the output of the equalizer becomes less than –40 dB compared to the signal energy (0 dB). However, this kind of spectral shaping of the noise signal causes biased estimation of the inverse of the channel. Biasedness of the estimation can be overcome by imposing some

restrictions on the adaptation equations. Since the objective here is to compare different types of error equations, we will not concentrate on this aspect now, and leave it for future study.

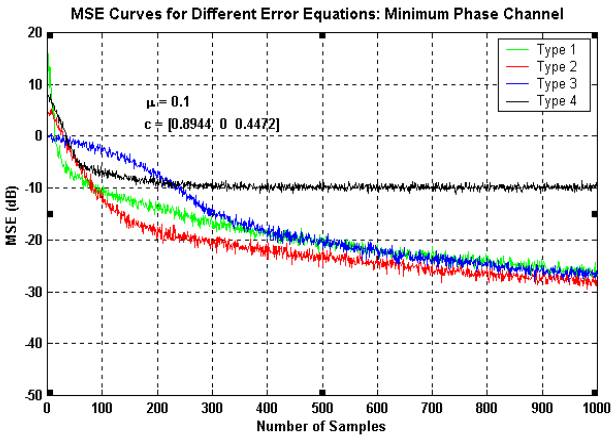

Figure 3.6: Zoomed Version of Figure 3.5.

From Figure 3.6 it is clear that, at the beginning of the adaptation process, the convergence rate is much faster for the equalizer with a Type1 error equation. But after ~50 samples, when the error is around –10 dB, the convergence rate with Type1 becomes slower than for the equalizer with a Type2 error. The reason for this is the non-symmetric behavior of a Type1 equation around zero error (Figure 3.2). Figure 3.2 shows that both Type2 and Type3 exhibit almost the same kind of symmetry around zero error. These two error equations provide almost the same value of error when $0.8 < |y(n)| < 1.2$. Consequently, the steady state MSE levels for these two Types are almost the same (Figure 3.5). Equalization with a Type3 error yields a slower convergence rate at the beginning, as expected from Section 3.1. The equalizer with a Type 4 error, even though it has a moderately good convergence rate at the beginning, produces a much higher steady state noise level. This result is also as expected from Section 3.1.

3.3.2 Exponentially Decaying Channel

The channel impulse responses, both in baud space and in fractional space, are shown in Figure 3.7. The decay time constant of the channel is one. The channel was normalized for unit energy. Other than the channel, the other simulation parameters are the same as those

used in Section 3.3.1. A delay of one symbol was used while initializing the equalizer coefficients. The MSE curves for the exponentially decaying channel for different types of error equation are shown in Figure 3.8.

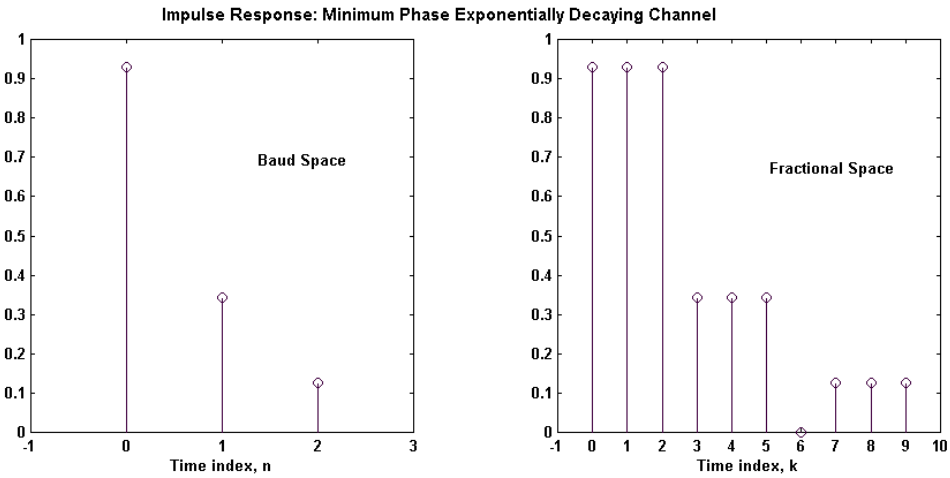

Figure 3.7: Impulse Response of the Exponentially Decaying Channel.

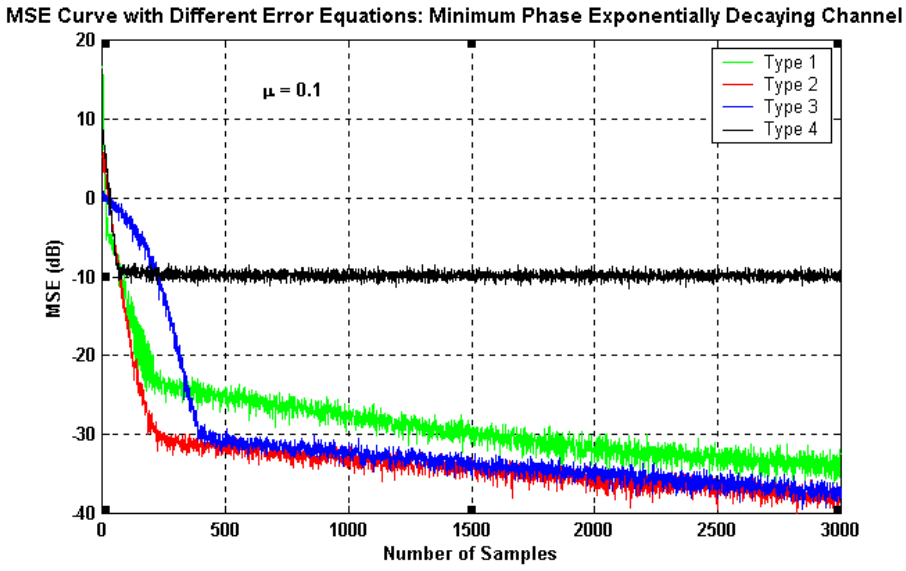

Figure 3.8: MSE Curves of the Equalizer with Different Error Equations for the Exponentially Decaying Channel.

Figure 3.8 shows almost the same effects of the different errors on the convergence rate of the equalizer as shown in Figure 3.5.

3.3.3 Symmetric Channel

The impulse response of the channel is described by a cosine function [7] as:

$$h(n) = \begin{cases} \frac{1}{2}\left[1+\cos\left(\frac{2p}{W}(n-1)\right)\right], & n = 0,1,2 \\ 0 & \text{else} \end{cases} \tag{3.27}$$

The parameter W controls the amount of amplitude distortion produced by the channel, with the distortion increasing with W. Eventually W controls the eigenvalue spread of the correlation matrix of the tap inputs to the equalizer, with the eigenvalue spread increasing with W. W = 3.1 is used in the simulation. In the simulation, $h(n)$ was normalized to have unit energy so that,

$$\sum_n h^2(n) = 1 \tag{3.28}$$

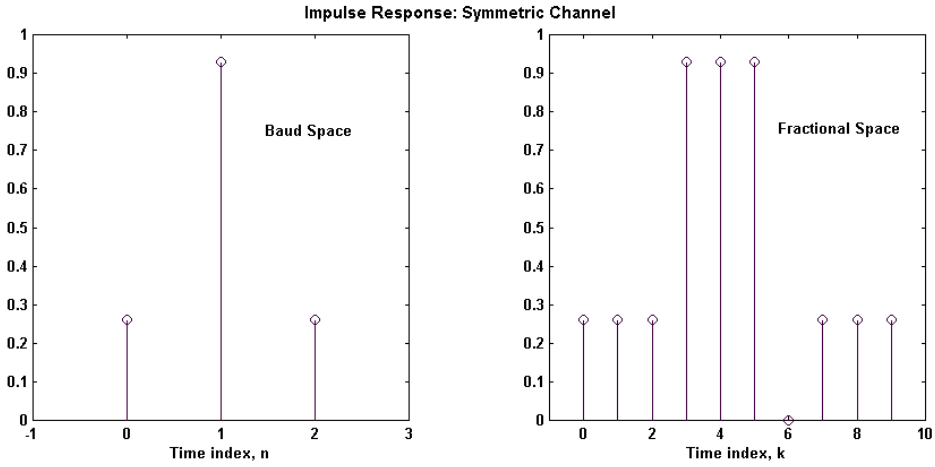

Figure 3.9: Impulse Response of the Symmetric Channel.

The impulse response of the channel, in baud space and in fractional space, is given in Figure 3.9. Due to the symmetry property, the channel introduces a group delay of one symbol. Therefore, unlike with the previous two channels, instead of using a one symbol system delay, a two-symbol system delay was considered during the initialization of the equalizer coefficients. The other parameters in the simulation were the same as those in the

previous two cases. For the symmetric channel the MSE curves of the equalizer adaptation process for different types of error are shown in Figure 3.10.

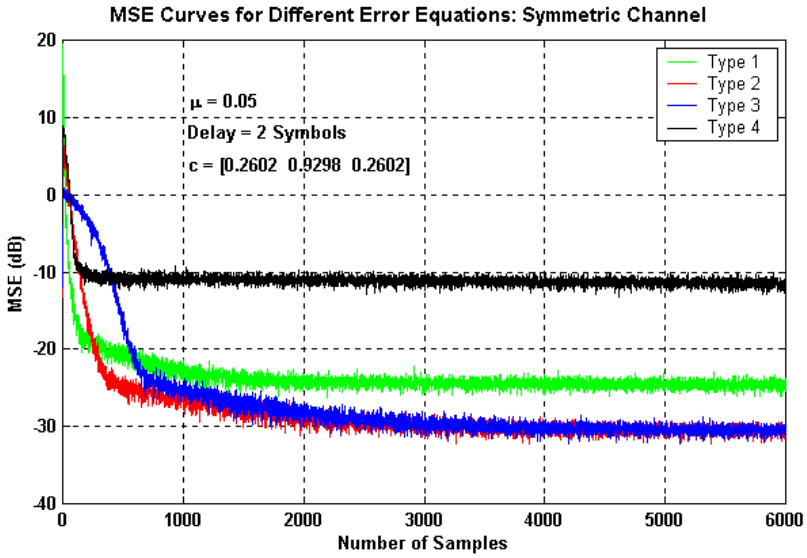

Figure 3.10: MSE Curves of the Equalizer with Different Error Equations for the Symmetric Channel.

From Figure 3.5, Figure 3.8, and Figure 3.10 we conclude that the Type2 error equation provides the optimal solution for the blind equalizer. This is because the system with a Type2 error equation yields a faster convergence rate than the system with a Type3 or Type4 error equation. Again Type2 results in a lower steady state error for a specific external noise. The problem with a Type2 error (and also with a Type3 error) is that, for some channels, the estimate of the equalizer (inverse of the channel) may be biased. To make the solution unbiased some kind of constraints need to be used while minimizing the cost function.

3.4 Effect of Adaptation Step Size

In Section 3.3 it has been shown that the steady state error of CMA with Type1 error is higher than the steady state error with Type2 or Type3. However the steady state error is a function of the adaptation step size m and the same m will not act similarly for different error types because of the unequal lumped constants of equations (3.10), (3.13), (3.16) and (3.21). Since all the results for different error equations shown in Section 3.3 were generated for the

same adaptation constant m, confusion may arise as to whether the different steady state errors are the result of using the same m for different error types or the result of the error types. To remove this confusion another simulation was performed with Type1 and Type2 error. In this simulation, different values of the adaptation step size were chosen for different error types so as to get the same convergence rate in each case. The step size used with Type1 error was 0.05 and that used with Type2 error was 0.1. The symmetric channel of Figure 3.9 was used for this simulation. All other parameters of the simulation were the same as those used to generate Figure 3.10. The simulation results are shown in Figure 3.11.

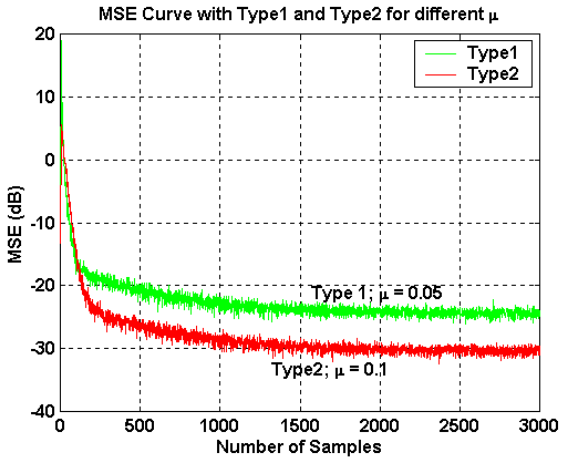

Figure 3.11: MSE Curve for Type1 and Type2 Error with Same Convergence Rate.

Figure 3.11 shows that even though both error types provide almost the same initial convergence rate, the Type2 error results in better steady state performance. As described earlier, the symmetric nature of the Type2 error about zero error causes this error equation to perform better than Type1, which is not symmetric about zero error.

Figure 3.12 shows the MSE curves of the adaptation process with Type2 error for different step sizes m. From Figure 3.12 it is clear that while the step size determines the convergence rate of the adaptation process, it does not have a significant effect on the steady state behavior. Therefore, it can be concluded that the steady state error of CMA mainly depends on the type of error equation used in the adaptation process and on the external noise level of the system.

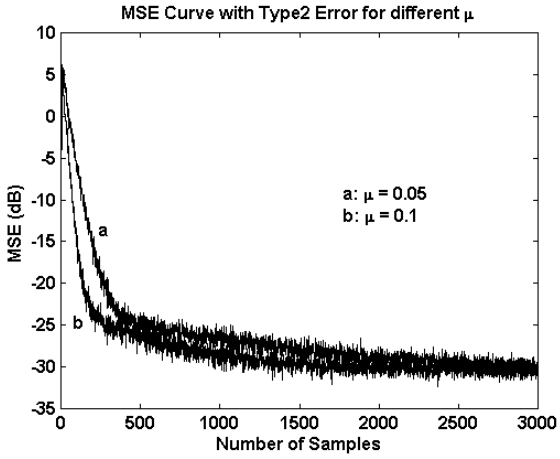

Figure 3.12: MSE Curve with Type2 Error for Different Step Size.

3.5 Effect of Symmetry About Zero Error

When an error equation is symmetric about the zero error or symmetric in the region of the global minima, the adaptive algorithm with this error equation corrects the equalizer coefficients, up or down equally, depending on the amplitude of the deviation. In this case the sign of the deviation determines only the direction, not the magnitude, of the correction. If the error is not symmetric about the zero error, it will result in different amounts of correction for the same amount of amplitude deviation depending on the direction (sign) of the deviation. For this reason the symmetric error types are expected to exhibit better steady-state performance. A simulation was performed to show the effect of the symmetric property of the error equation on the steady state performance of the adaptive system. Type1, Type2 and Type3 error equations with correction factors are used in the simulation. The corrected equations are given below.

$$\begin{aligned}
&\text{Type1c}: \; e(n) = \frac{1}{2A}\left(|y(n)|^2 - A^2\right) \\
&\text{Type2c}: \; e(n) = |y(n)| - A \\
&\text{Type3c}: \; e(n) = A\ln\left(\frac{|y(n)|}{A}\right)
\end{aligned} \tag{3.29}$$

The corrections were made to make all the error equations have the same slope at the zero error point. Since the corrections will change the lumped constants of the weight update

equations, equations (3.22), (3.23) and (3.24) were used with the corrected error equations without any change. The symmetric channel (Figure 3.9) was used in the simulation. The simulation result for the adaptation step size of 0.1 (m = 0.1) is shown in Figure 3.13. All other parameters are the same as those used for generating Figure 3.10. The signal to noise ratio used in the simulation is 40 dB. 500 different realizations were performed with independent input sequences and the results of those experiments were averaged to generate the curves of Figure 3.13. The same simulation was also performed with the different adaptation step size m = 0.2 and the results of this experiment are shown in Figure 3.14. Fifty different realizations were used to plot the curves of Figure 3.14.

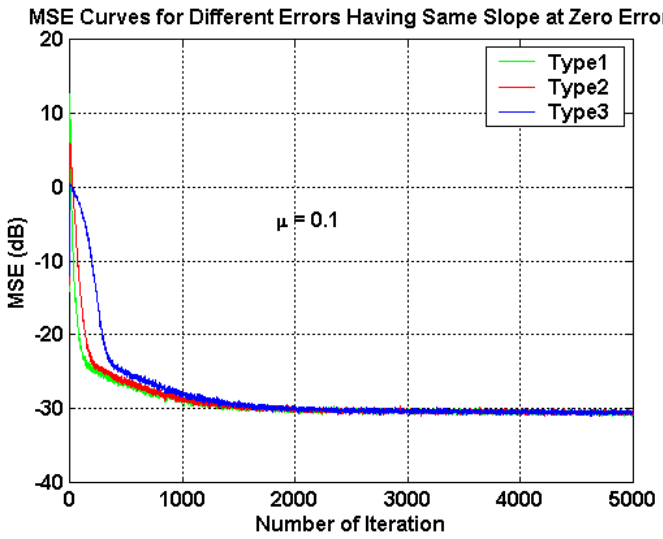

Figure 3.13: MSE Curves for Different Error with Same Slope at Zero Error (m = 0.1).

Figure 3.13 shows that the steady state MSE levels of the adaptation process with different error equations are almost the same while Figure 3.14 shows a different steady state error level for different errors. Figure 3.14 also shows that Type1, even after correction for the slope, performs worst in terms of steady state MSE, among the three error types used in the simulation. The reason for this poor performance is the non-symmetric behavior of the Type1 error. For a small adaptation step size, the non-symmetric behavior of the error equations becomes insignificant and thus Figure 3.13 does not show any difference in steady state behavior of the adaptation process with different error types.

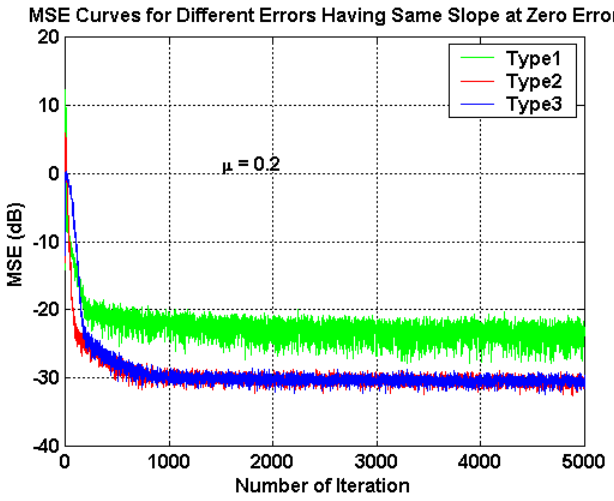

Figure 3.14: MSE Curves for Different Error with Same Slope at Zero Error (m = 0.2).

3.6 Effect of Initialization

In the previous chapter (Section 2.3), it was mentioned that in a blind adaptation scheme, the initialization of the equalizer coefficients determines whether the equalizer will converge to a global minimum or to a local minimum. In this section we will show that the convergence to a global or a local minimum not only depends on the initialization but also on the type of error equation that is used in the adaptation process. To show the effect of the initialization we will simulate the same system as used in Section 2.3 but with different types of error equation. The simulated system is shown in Figure 2.4. The system has a single pole channel with a transfer function given by,

$$C(z) = \frac{1}{1 + 0.7z^{-1}} \tag{3.30}$$

A baud spaced FIR equalizer of length 2 will be used to nullify the effect of the channel on the received signal. It is clear from (3.30) that, to converge to the correct minimum point, the equalizer coefficient vector should have the value of **f** = [1 0.7]. If a differential encoding scheme is used, **f** = [-1 -0.7] would also be an acceptable solution. Therefore, in the equalizer space (**f**-space), the positions of the acceptable or global minima are ±[1 0.7]. If the adaptation process causes the equalizer to converge to some other points

in **f**-space, those points will be considered to be local minima since those values of equalizer coefficients do not provide a correct (or acceptable) solution to the problem.

Similar to Section 2.3, the effect of the initialization on the convergence behavior will be observed by initializing the equalizer coefficients with 20 different points in **f**-space. These 20 points are selected such that they all are equally spaced and lying on a circle of radius 2. The same input sequence of length 4000 will be used for all the different initialization situations. An adaptation step size of 0.005 (m = 0.005) was used in the simulations. The simulation results for different types of error are shown below.

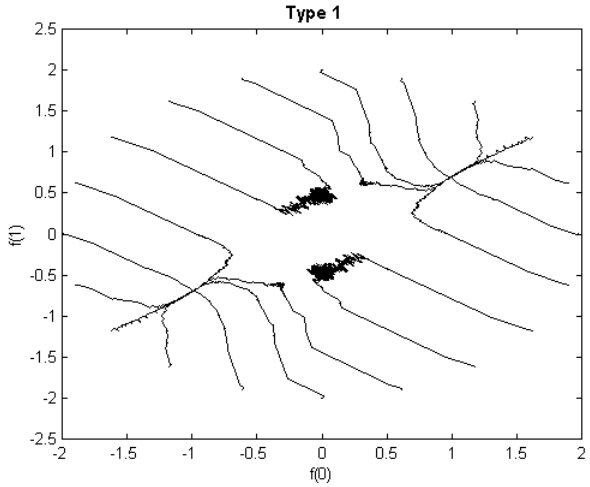

Figure 3.15: Effect of Initialization on Blind Equalization with Type1 Error.

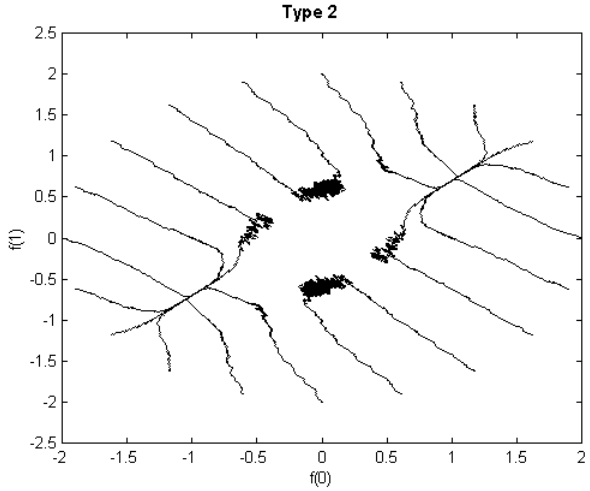

Figure 3.16: Effect of Initialization on Blind Equalization with Type2 Error.

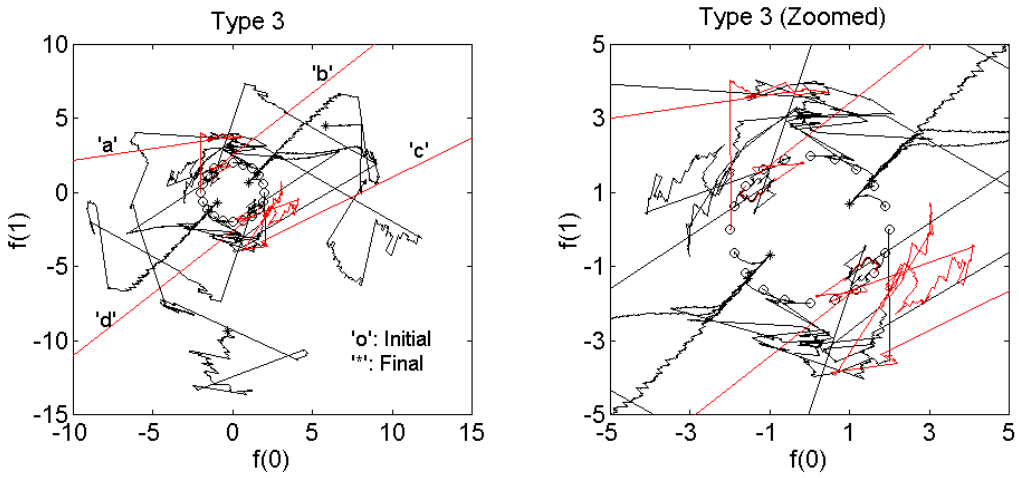

Figure 3.17: Effect of Initialization on Blind Equalization with Type3 Error.

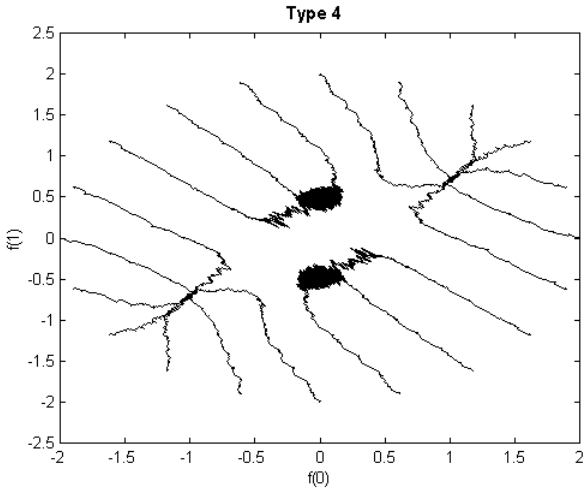

Figure 3.18: Effect of Initialization on Blind Equalization with Type4 Error.

Figure 3.15, Figure 3.16, Figure 3.17, and Figure 3.18 show the effect of initialization on the convergence behavior of a blind equalizer for error Type 1, 2, 3, and 4 respectively. These figures show that for all the error types, except for the Type3 case, convergence to global minima depends on the initialization. These figures also seem to show that the probability of converging to local minima is higher for a system with a Type4 error equation.

In Figure 3.17 the circles ‘o’ indicate the initial points and the asterisks ‘*’ indicate the final value of the equalizer coefficients after 4000 iterations. From Figure 3.17 it is clear that Type3 error exhibits a completely different property than the other error types. Figure

3.17 shows that with a Type3 error and a differentially encoded source, the equalizer will always converge to the global minima, irrespective of the initialization of the equalizer. However, the Type3 simulation results also show problems with convergence of the equalizer (cases a, b, c, and d in Figure 3.17). The diverging behavior of the equalizer with Type3 error can be explained from the error equation and the weight update equation, which are given below.

$$e(n) = \ln\left(\frac{|y(n)|}{A}\right)$$
$$\mathbf{f}(n+1) = \mathbf{f}(n) - me(n)\frac{\mathbf{x}(n)}{y(n)} \tag{3.31}$$

From (3.31) it is clear that if for any reason the output $y(n)$ becomes negligible, this will render the error $e(n)$ very large ($e(n) = -\infty$ for $y(n) = 0$). In the weight update equation $y(n)$ appears in the denominator. Therefore, if $y(n)$ becomes too small, the equalizer coefficient vector will be updated by a large correction. As a consequence of these two facts, the equalizer will start to diverge. To avoid divergence of the equalizer, the Type3 error equation will be modified as follows:

1. Use a hard-limiter at the output of the equalizer. The hard-limiter will not allow the output amplitude of the equalizer to go below a certain level. In the simulation, since the desired amplitude level of the output signal was 1, this level was set to 0.01.

2. To avoid a very high value of error for a small value of output amplitude, and also to make the error equation symmetric about zero error, the error equation will be modified to:

$$e(n) = \begin{cases} \ln\left(\dfrac{|y(n)|}{A}\right), & \text{for } |y(n)| \geq A \\ -\ln\left(\dfrac{2A - |y(n)|}{A}\right), & \text{for } |y(n)| < A \end{cases} \tag{3.32}$$

The modified Type3 error equation and the original Type3 error equation are shown in Figure 3.19. The effect of initialization with the modified Type3 error equation is shown in Figure 3.20. The same simulation parameters were used to generate the plots of Figure 3.20 as were used for generating Figure 3.17. The same weight update equation (3.31) was used for the modified Type3 error equation.

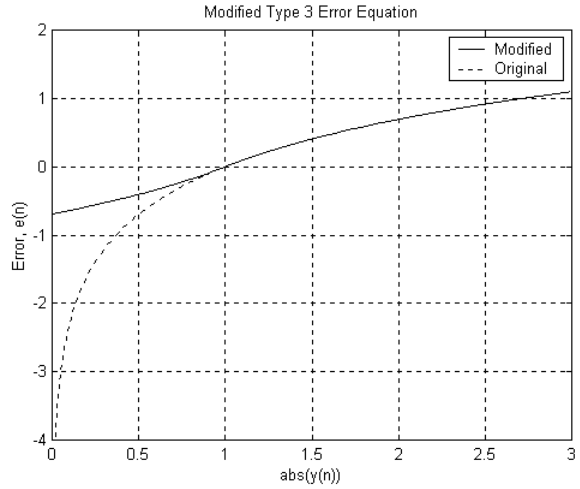

Figure 3.19: Modified Type 3 Error Function.

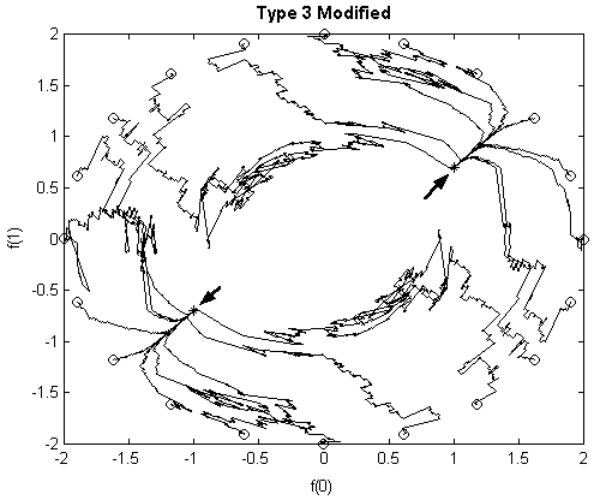

Figure 3.20: Effect of Initialization on Blind Equalization with Modified Type 3 Error.

Similar to Figure 3.17, in Figure 3.20 the ‘o’s indicate the initial and the ‘*’s indicate the final values of the equalizer coefficients. The arrows in Figure 3.20 show the positions of the global minima. It is clear from Figure 3.20 that, after the modifications, a Type3 error equation will always lead the equalizer to converge to a global minimum and thereby

eliminate the dependency of the convergence behavior on the initialization. Since, irrespective of the initialization, the equalizer always converges to the global minima, it can be expected that the modified Type3 error equation provides a cost surface with no local minimum.

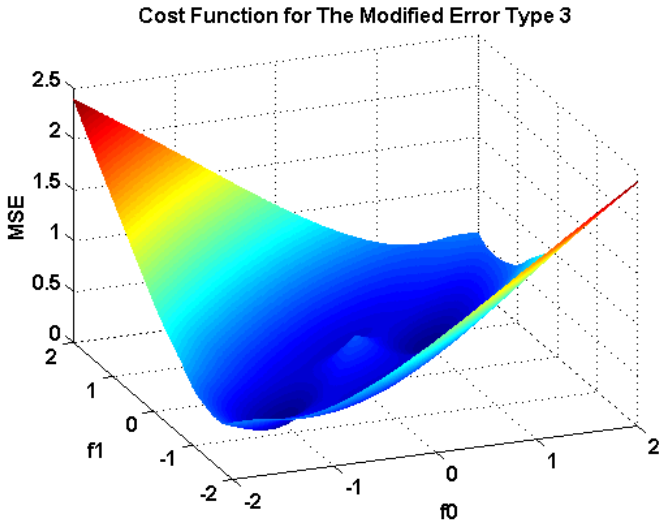

Figure 3.21: Cost Surface of CMA with Modified Type3 Error.

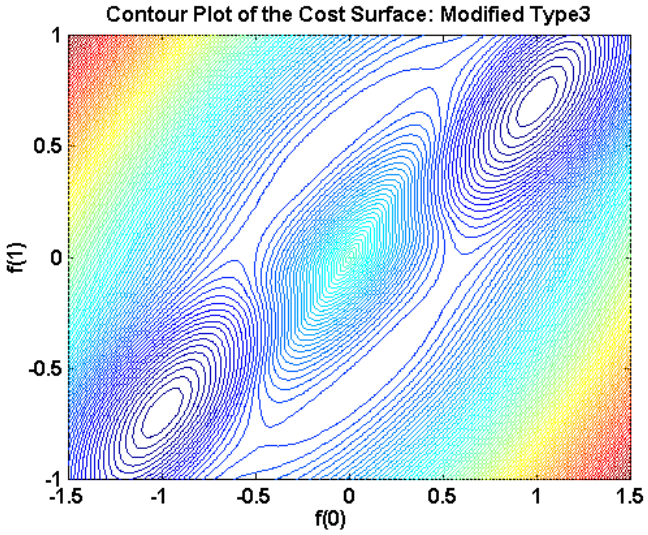

Figure 3.22: Contour Plot of the Cost Surface of Figure 3.21.

The cost surface and the contour plot of the cost surface of CMA with Modified Type3 error are shown in Figure 3.21 and Figure 3.22 respectively. Both representations of the cost surface (Figure 3.21 and Figure 3.22) confirm the absence of local minima in the cost surface of CMA with Modified Type3 error.

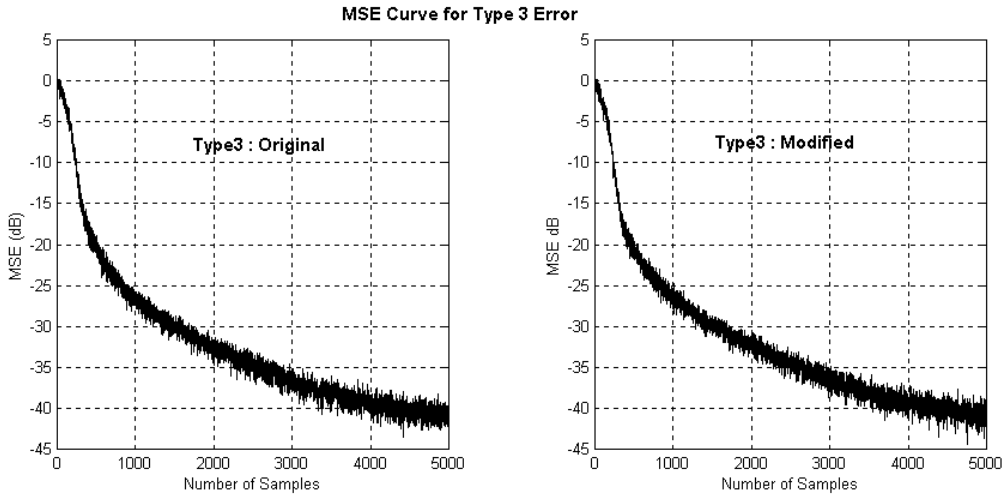

Figure 3.23: MSE Curves of the FSE with Type 3 Error and Modified Type3 Error for the Minimum Phase Channel (Figure 3.4); m=0.1.

To see how the modification of the Type 3 error affects the convergence rate of the equalizer, a FSE of length 12 was adapted using the modified error equation for the minimum phase channel shown in Figure 3.4. The value of the adaptation step size used in the simulation was 0.1. The same experiment was performed in Section 3.3.1 with the original Type3 error. Both MSE curves are shown in Figure 3.23. Figure 3.23 shows that the modifications made to the Type3 error equation do not seem to have any effect on the convergence rate or the steady state MSE of the equalizer.

Based on the simulation results we conclude that the equalizer with a Type2 error equation exhibits better convergence rate than with any other type of error. A Type3 error yields better results than the other error types in the sense of always converging to the global minima. Even though we have better performance with the Type2 or modified Type3 error equation, a Type1 error equation will be used in the next chapter to design a new blind equalizer. This is done only to facilitate ease of comparison, because the Type1 error is commonly used in conventional blind equalizers.